

High-Performance Supercapacitors from Niobium Nanowire Yarns

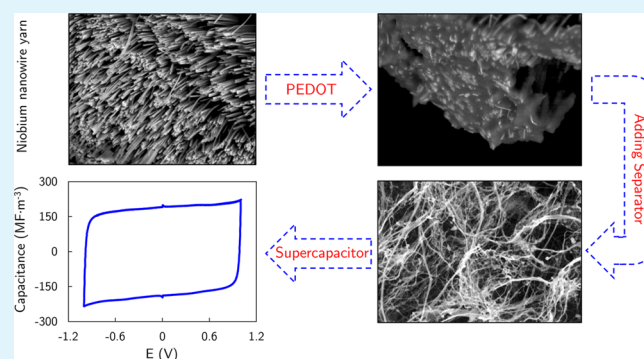
Seyed M. Mirvakili,^{*,†} Mehr Negar Mirvakili,[‡] Peter Englezos,[‡] John D. W. Madden,[§] and Ian W. Hunter[†][†]Department of Mechanical Engineering, BioInstrumentation Laboratory, Massachusetts Institute of Technology, Cambridge, Massachusetts 02139, United States[‡]Department of Chemical and Biological Engineering, University of British Columbia, Vancouver, BC V6T 1Z3, Canada[§]Department of Electrical and Computer Engineering, Advanced Materials and Process Engineering Laboratory, University of British Columbia, Vancouver, BC V6T 1Z4, Canada

Supporting Information

ABSTRACT: The large-ion-accessible surface area of carbon nanotubes (CNTs) and graphene sheets formed as yarns, forests, and films enables miniature high-performance supercapacitors with power densities exceeding those of electrolytics while achieving energy densities equaling those of batteries.^{1–7} Capacitance and energy density can be enhanced by depositing highly pseudocapacitive materials such as conductive polymers on them.^{3,8–15} Yarns formed from carbon nanotubes are proposed for use in wearable supercapacitors.^{3,16} In this work, we show that high power, energy density, and capacitance in yarn form are not unique to carbon materials, and we introduce niobium nanowires as an alternative. These yarns show higher capacitance and energy per volume and are stronger and 100 times more conductive than similarly spun carbon multiwalled nanotube (MWNT) and graphene yarns.^{6,17–22}

The long niobium nanowires, formed by repeated extrusion and drawing,¹⁷ achieve device volumetric peak power and energy densities of 55 MW·m⁻³ (55 W·cm⁻³) and 25 MJ·m⁻³ (7 mWh·cm⁻³), 2 and 5 times higher than that for state-of-the-art CNT yarns, respectively.³ The capacitance per volume of Nb nanowire yarn is lower than the 158 MF·m⁻³ (158 F·cm⁻³) reported for carbon-based materials such as reduced graphene oxide (RGO) and CNT wet-spun yarns,⁵ but the peak power and energy densities are 200 and 2 times higher, respectively.⁵ Achieving high power in long yarns is made possible by the high conductivity of the metal, and achievement of high energy density is possible thanks to the high internal surface area. No additional metal backing is needed, unlike for CNT yarns and supercapacitors in general, saving substantial space. As the yarn is infiltrated with pseudocapacitive materials such as poly(3,4-ethylenedioxythiophene) (PEDOT), the energy density is further increased to 10 MJ·m⁻³ (2.8 mWh·cm⁻³). Similar to CNT yarns, niobium nanowire yarns are highly flexible and show potential for weaving into textiles and use in wearable devices.

KEYWORDS: supercapacitors, energy storage, metal nanowires, niobium nanowires, PEDOT, flexible capacitors, yarn nanowires, cellulosic separators



INTRODUCTION

A lack of biocompatibility of carbon nanoparticles limits their application in biomedical devices and implants. Niobium, which is more abundant than molybdenum, silver, and tin and is widely used in steel alloys, is by nature a highly chemically stable, hypoallergenic, biocompatible, and bioinert material,²³ which makes it appropriate for applications in jewelry and biomedicine and for use in corrosion-resistant coatings for surgical tools. The volumetric capacitance of bare niobium nanowire yarns is measured to be 3 times higher than that of carbon nanotube yarns. This combination of high electrical conductivity and high volumetric capacitance makes possible the high power and energy densities for bare niobium nanowire (Nb NW) yarns. Although their energy density is lower than in some graphene and activated carbon electrodes, these materials

cannot achieve the same power density without the use of a metal backing layer, thereby losing their advantage.⁵

In this work, we have measured the electrochemical properties of Nb NW yarns and evaluated their performance as supercapacitor electrodes. Electrochemical characteristics of bare Nb NW yarns are reported in various electrolytes. A highly ionically conductive cellulose-based separator was designed for use in the supercapacitor. To boost the performance, we deposited the conducting polymer poly(3,4-ethylenedioxythiophene) (PEDOT) on the electrodes and measured the device performance. For the purpose of demonstration, a bare Nb NW-based supercapacitor is shown to harvest energy from a

Received: March 16, 2015

Accepted: June 12, 2015

Published: June 12, 2015

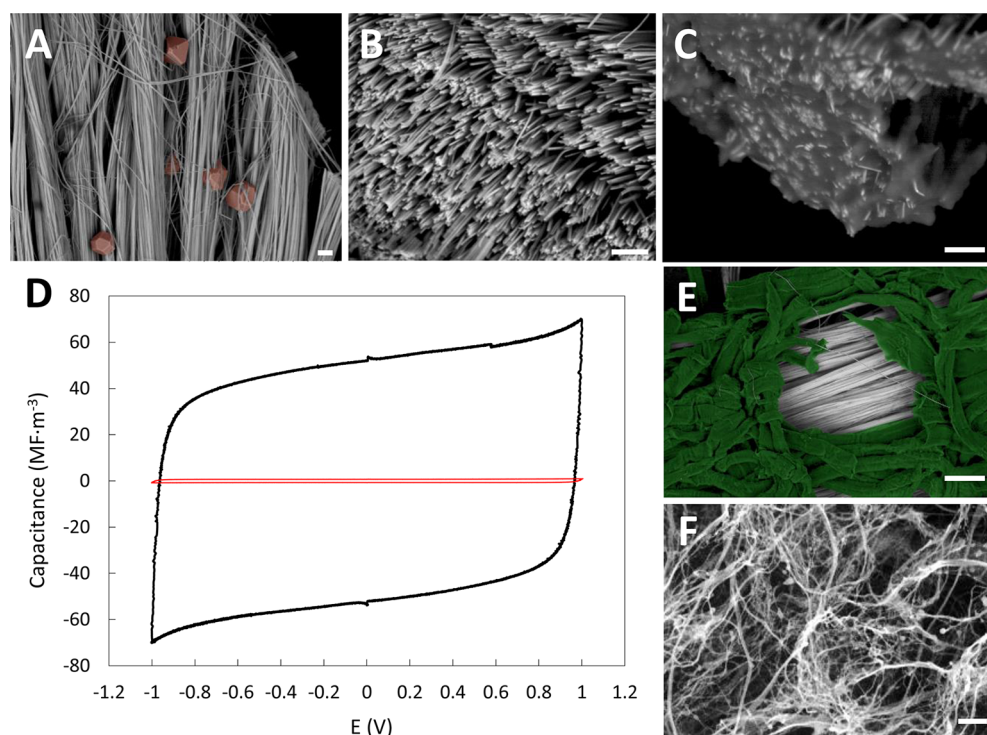


Figure 1. (A) SEM image of niobium nanowire yarn shows unetched copper microparticles during the copper etching process. (B,C) SEM images of copper-free niobium yarn before and after PEDOT deposition, respectively. (D) The increase in volumetric capacitance (with units of $\text{MF}\cdot\text{m}^{-3}$ or $\text{F}\cdot\text{cm}^{-3}$) of one electrode from depositing PEDOT (black line) on bare Nb nanowires (red line) at a scan rate of $500\text{ mV}\cdot\text{s}^{-1}$. To demonstrate that the cell is perfectly symmetrical, we performed the CV from -1 to 1 V. The glitches at the zero potential are due to the artifact of the measurement device. (E) Thin paper (Kimwipe), as a separator, showed poor performance. (F) High-performance separators were prepared by cellulosic wood pulp fibers of different sizes. Scale bars for all SEM images are $5\ \mu\text{m}$ except for (E), which is $20\ \mu\text{m}$.

solar cell and then to energize a temperature sensor and an FM transmitter (as shown in the Supporting Information).

RESULTS AND DISCUSSION

The niobium nanowires, seen in parts A and B of Figure 1, are twisted into yarns (as seen in Figure S1 in the Supporting Information), forming high internal surface area materials (100 times the area of Ni foam)²⁴ whose individual strands are 140 nm in diameter. To estimate the specific capacitance expected of the Nb NW yarns, we measured the capacitance per area (C_A) of bulk niobium and found it to be $0.52\ \text{F}\cdot\text{m}^{-2}$ ($52\ \mu\text{F}\cdot\text{cm}^{-2}$) (as detailed in the methods section). Using the value for C_A and the 140 nm average diameter of the Nb NW yarns, an estimated specific volumetric capacitance limit of $1.36 \times 10^7\ \text{F}\cdot\text{m}^{-3}$ ($13.6\ \text{F}\cdot\text{cm}^{-3}$) and gravimetric capacitance limit of $1.5\ \text{F}\cdot\text{g}^{-1}$ was found, which is lower than the gravimetric capacitance of carbon-based materials (see details in the Supporting Information). Capacitances of the Nb NW yarns were measured in aqueous, organic, and ionic liquid electrolytes (Table S1 in the Supporting Information). The highest capacitances and power densities were achieved in sulfuric acid solution. The experimental values were measured to be $1.1 \times 10^7\ \text{F}\cdot\text{m}^{-3}$ ($11\ \text{F}\cdot\text{cm}^{-3}$) and $1.3\ \text{kF}\cdot\text{kg}^{-1}$ ($1.3\ \text{F}\cdot\text{g}^{-1}$) for yarns made of nanowires with individual average diameters of 90 nm, which are close to the estimated limits, higher than the value of $0.5 \times 10^7\ \text{F}\cdot\text{m}^{-3}$ ($5\ \text{F}\cdot\text{cm}^{-3}$) for carbon nanotube yarns⁴ and close to the value of $1.2 \times 10^7\ \text{F}\cdot\text{m}^{-3}$ ($12\ \text{F}\cdot\text{cm}^{-3}$) reported for densely packed single-walled carbon nanotubes in organic electrolyte (i.e., Et_4NBF_4 and propylene carbonate).²⁵ Using ionic liquids allows higher operating voltages of up to 3 V. Capacitors of up to 36 mF are made with bare niobium

nanowires, and this value is higher than the largest capacitance value of 10 mF made with PEDOT-coated carbon nanotube yarns plied with Pt microwire.³ Although nanotubes have much smaller diameters, the capacitance per area is much smaller, and there is a tendency for bundling to occur, reducing the accessible surface area. For example, among carbon-based materials, graphene has the largest double layer capacitance of $0.21\ \text{F}\cdot\text{m}^{-2}$ ($21\ \mu\text{F}\cdot\text{cm}^{-2}$)^{26,27} but with a total capacitance of $0.065\ \text{F}\cdot\text{m}^{-2}$ ($6.5\ \mu\text{F}\cdot\text{cm}^{-2}$),²⁷ which is almost 10 times lower than that of niobium. This is explained by the fact that although the ion-accessible area is very high for graphene, the quantum capacitance (arising from the low density of states) is small. The niobium nanowires we used in this work do not suffer from this limitation, in part due to their relatively large diameter (approximately 90–140 nm), and capacitance is thus determined by the double layer.

The conductivity of Nb NW yarns was measured to be $3 \times 10^6\ \text{S}\cdot\text{m}^{-1}$ (as detailed in the methods section), which is 100 times higher than that in multiwalled carbon nanotube yarns ($3 \times 10^4\ \text{S}\cdot\text{m}^{-1}$).¹⁷ Nb NW yarns were infiltrated with electrodeposited PEDOT, as seen in Figure 1C, and bare nanowires shown in Figure S3 in the Supporting Information. For a 54 wt % sample, the volumetric capacitance was improved 70 fold (Figure 1) up to $5 \times 10^7\ \text{F}\cdot\text{m}^{-3}$ ($50\ \text{F}\cdot\text{cm}^{-3}$); the mechanism is described in Figure S1 in the Supporting Information). The gravimetric capacitance increased linearly with the PEDOT mass fraction, directly correlating to the deposition time (Figure S7 in the Supporting Information). The constant current charge and discharge response of a Nb NW yarn before and after coating with PEDOT is shown in Figure 2C. The charge and discharge time for the PEDOT-

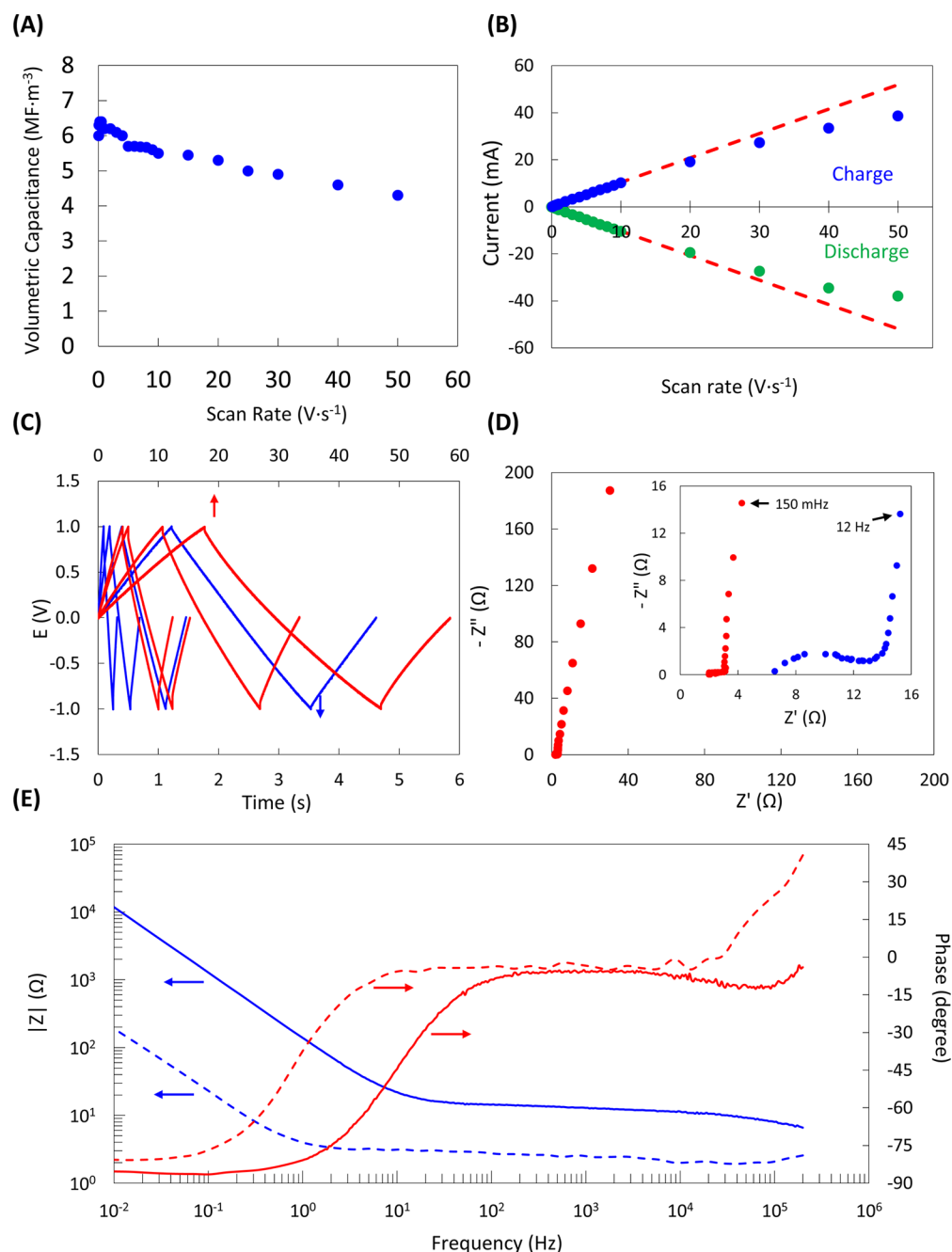


Figure 2. (A) Volumetric capacitance (with unit of MF·m⁻³ or F·cm⁻³) of bare Nb NW yarn (with an individual nanowire average diameter of 140 nm) as a function of the scan rate for a capacitor with a diameter of 85 μm per electrode and a separator thickness of 9 μm. (B) Scaling of the current (at 0 potential point) as a function of scan rate. At 20 V·s⁻¹, the current no longer increases in direct proportion to the scan rate. (C) Constant current charging and discharging of the supercapacitor before (blue, at 0.3, 1, 2, and 4 A·g⁻¹ from right to left, respectively) and after (red, at 0.9, 1.5, 3, and 3.7 A·g⁻¹ from right to left, respectively) depositing PEDOT (all per mass of dry electrode). (D) Nyquist plot of the PEDOT-coated supercapacitor (red); the inset shows the Nyquist plots for bare (blue) and PEDOT-coated (red) samples. (E) Bode plot of the supercapacitor before (solid line) and after (dashed line) PEDOT deposition.

coated sample increases, but still it shows a very capacitive response.

The combination of the high conductivity of the metal nanowires and the high volumetric capacitance of the filler provides an opportunity to achieve both high energy and high power densities. Various separators (such as glass fibers and Nafion and millipore membranes) were tested, and cellulosic-based thin sheets (made of micron-sized cellulosic wood pulp fibers) had the highest ionic conductivity (3.4 S·m⁻¹ in 1 M sulfuric acid), with an electrolyte uptake of up to 600% (details

given in the Supporting Information). Having a highly ionically conductive separator reduces the equivalent series resistance, and this directly increases the power density. Due to the hydrophilicity and exceptionally high tensile strength of microfiber cellulose film-based materials, they are an excellent candidates for use in high-power-storage devices.²⁸

Wrapping gold or platinum microwires around the infiltrated yarn as charge collectors has resulted in great improvements in power density for supercapacitors made with CNT yarns coated with conducting polymers.³ No external charge collector wires

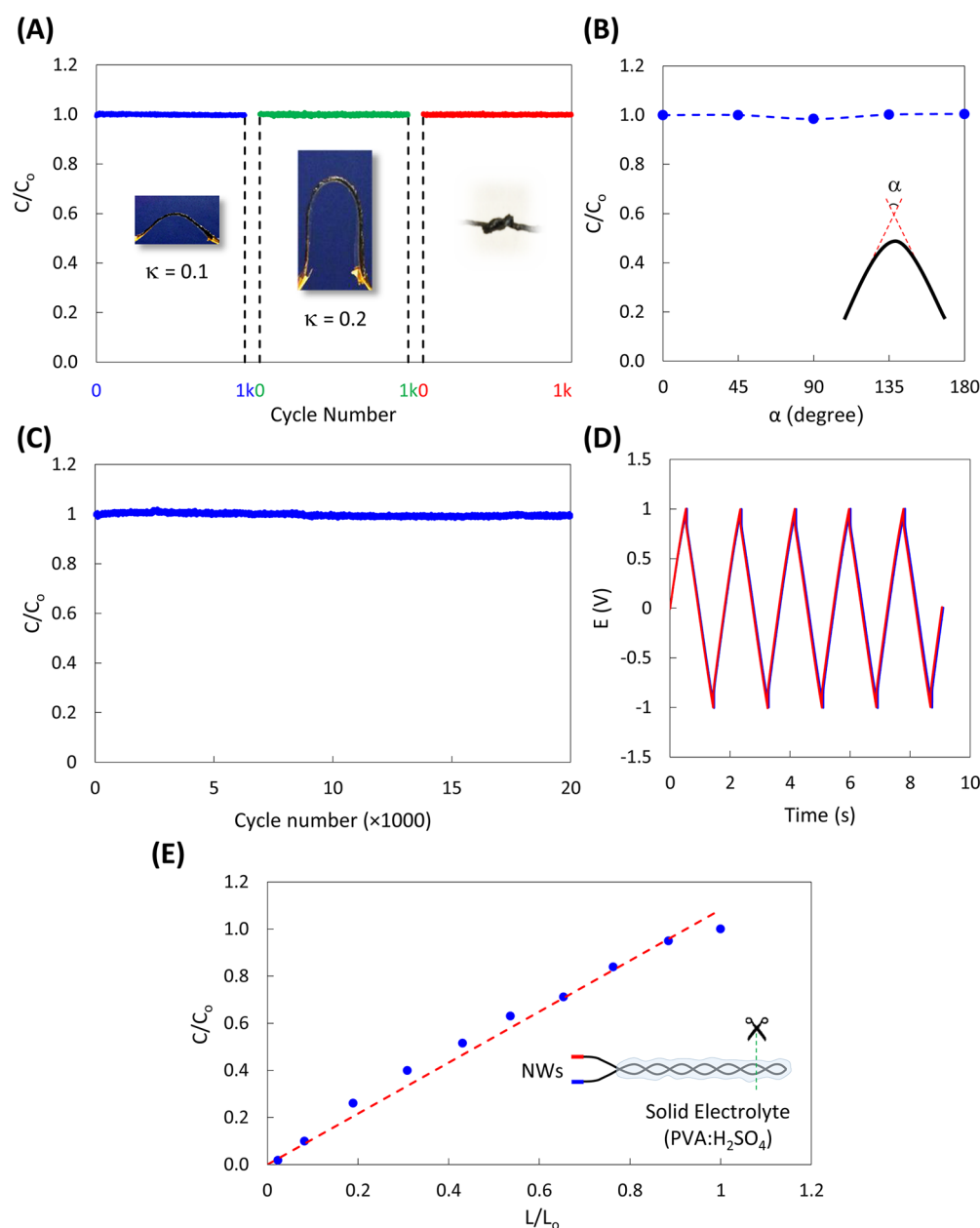


Figure 3. (A) Performance of the solid-based supercapacitor with a length of 50 mm and diameter of 140 μm under different deformation states, measured for 1000 cycles sequentially from left to right. The unit for curvature is $(\text{mm})^{-1}$. (B) The sample was then bent at increasing angles, and the performance was measured again. (C) A life cycle test of a sample in 2 M sulfuric acid performed using 10 mA for 20 000 cycles. (D) First (blue) and last (red) 5 cycles of constant current charge and discharge test for the 20 000 life cycle test. In these experiments, one cycle is considered to be one full charge and discharge from 0 to 1 to 0 V. (E) Capacitance versus length. One 40 mm long supercapacitor made with solid electrolyte was shortened in 4 to 5 mm increments, and its capacitance was measured at each step.

are used in the niobium device-performance evaluations because the Nb nanowire yarns already have a high conductivity (details given in the Supporting Information). Due to the high conductivity of the electrolyte, the separator, and the electrode itself, Nb NW supercapacitors showed great performance at fast charging rates with relatively little loss of capacitance as the scan rate is increased to $50 \text{ V}\cdot\text{s}^{-1}$ (parts A and B of Figure 2).

To evaluate the scalability of the device, we measured the volumetric capacitance as a function of the diameter and inserted twist (see the Supporting Information). As the diameter increases approximately 3.5 fold, the volumetric capacitance only decreases by a factor of approximately 1.5, which is much less than the value reported for PEDOT-coated

CNT yarns (a decrease of volumetric capacitance by a factor of 2 for an increase in diameter by a factor of 1.4).³ Capacitance as a function of twist shows <10% decreases in capacitance when the twist is increased from 0 to close to the breaking point (details given in the Supporting Information).

Electrochemical impedance spectroscopy was performed (details given in the methods section) to measure the equivalent series resistance (ESR) and the frequency response of the supercapacitor (Figure 2D,E). An ESR of 2Ω was achieved in aqueous electrolyte (1 M sulfuric acid). The electronic resistance of the 60 mm long metal nanowires is of a similar magnitude, suggesting that this, perhaps combined with the separator resistance, is determining the ESR. A carbon

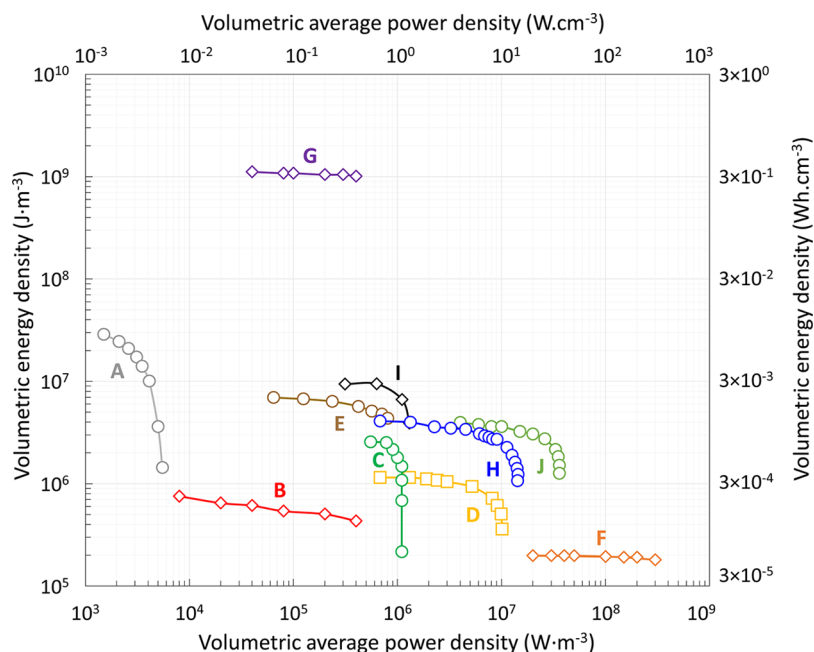


Figure 4. Ragone plots comparing volumetric energy and power densities. (A) A 4 V, 500 μAh Li thin-film battery.³⁰ (B) A MnO_2 carbon fiber supercapacitor.³¹ (C) A 2.75 V, 44 mF activated carbon electrochemical capacitor.²⁶ (D) A 3.5 V, 25 mF supercapacitor.³⁰ (E) A 2.7 V, 1F Maxwell supercapacitor. (F) A 63 V, 220 μF electrolytic capacitor.³⁰ (G) A Panasonic (17 500) Li-ion battery.¹ (H) This work: bare Nb NW yarn supercapacitor in ionic liquid (tetraethylammonium tetrafluoroborate in propylene carbonate (1M)) operating at 3 V. (I) This work: PEDOT-coated Nb NW yarn supercapacitor. (J) A two-ply CNT/PEDOT electrode supercapacitor.³ Data for this work are shown with labels I and H; the rest are extracted from the references mentioned.

multiwalled nanotube yarn of the same dimensions without a collector would have a resistance approximately 100 times larger, a similar capacitance, and thus 100 times slower charging. The absence of an additional charge collection layer is an important advantage of using a nanostructured metal electrode (rather than relatively poorly conductive carbon) and reduces the contact resistance. For the samples made with a solid electrolyte, the ESR is twice that of the liquid-based supercapacitor (shown in the Supporting Information). The dominant time constants are 30 ms for the metal nanowire and 200 ms when it is PEDOT-infiltrated. An impedance model for the supercapacitor was found and is presented in the Supporting Information.

Bending and Life Cycle Tests. The ultimate tensile strength of twisted niobium nanowire yarns can be as high as 1.1 GPa,¹⁷ which is higher than that of twisted carbon nanotube yarns and graphene yarns.^{18–20,29} This property, combined with its excellent flexibility, make Nb NWs an interesting candidate for integration into fabrics. To test the ability of the devices to bend, twist, and knot, we made a solid electrolyte-based supercapacitor for the flexibility tests. The performance was measured at different deformation states, and the results (Figure 3A) show almost no change in the performance with bending and knotting. Bending tests were also performed to evaluate the flexibility of the device, it showing almost no changes in capacitance when bent from 0 to 180° (Figure 3B).

The life cycle was measured by using a constant current charge and discharge technique. The capacitance was almost fully retained over 20 000 cycles, with the capacitance as a function of the cycle number shown in Figure 3C. Coulombic (or equivalently Faradaic) efficiency is close to unity through the 20 000 cycles performed (Figure S9 in Supporting Information). Figure 3D shows that the first and last ten cycles of constant current charge and discharge almost

completely match, indicating no loss of performance at the end of the life cycle test.

One solid electrolyte-based supercapacitor was cut from the end, and the capacitance was measured, showing a linear relationship between length and capacitance (Figure 3E). This indicates that the supercapacitor structure is contributing to the capacitance uniformly along the length.

Energy Density and Power Density. The peak power density and energy density of $55 \text{ MW}\cdot\text{m}^{-3}$ ($55 \text{ W}\cdot\text{cm}^{-3}$) and $25 \text{ MJ}\cdot\text{m}^{-3}$ ($7 \text{ mWh}\cdot\text{cm}^{-3}$) were measured for a supercapacitor made from two bare niobium nanowire electrodes with separator (full device), which is higher than that measured for the ultrafast charging supercapacitors with CNT, PEDOT, and gold as shown in Figure 4³ (see the methods section for details of the calculations). However, the average power density (Figure 4H,I) is lower than the average power density of the CNT, PEDOT, and gold. CV curves scanning from 0 to 3 V for the bare niobium yarns and PEDOT-coated Nb NW yarns (Figures S4 and S5 in the Supporting Information) were used to calculate the data points as described in the methods section. The high capacitance and energy densities are the result of the high surface capacitance of niobium relative to carbon, and compensate for the relatively large diameter of the niobium employed in this study (140 nm compared to 10 nm in carbon multiwalled nanotubes).

CONCLUSIONS

In this work, we demonstrated that niobium nanowire electrodes achieved performance levels similar to those of carbon nanotube- and graphene-based devices. The high conductivity of niobium, its good mechanical properties, and its high surface capacitance make this metal a viable alternative to carbons.

Due to the fast charging capabilities of the capacitor, niobium is appropriate for circuits where high current pulses are required. For demonstration purposes, a 36 mF supercapacitor was made with bare Nb nanowires (with ionic liquid electrolyte) and was used to store energy from a solar cell every 10 s and then release it to a 30 mW FM transmitter with a minimum operating voltage of 2.5 V. A video (shown in the Supporting Information) is taken after 10 000 cycles. Due to the flexibility of the electrodes, this device can be integrated into systems without imposing any design or dimension constraints.

METHODS

The niobium nanowires are extracted from copper–niobium composite wires as described in reference 17. Identical electrodes are then made from the resulting niobium nanowires by adding a small amount of twist to each yarn.

Cellulosic-based thin sheets were used as the separator and electrolyte absorber. The micron-sized cellulosic wood pulp fibers were obtained by refining kraft softwood pulp from a mill in Central British Columbia. Different fiber sizes were collected at different refining energies. The average fiber size in pulp suspension was measured by a Scircro Malvern 2000 Mastersizer. The separator sheets were prepared using the pulps with four different fiber sizes: 977, 560, 340, and 177 μm . The sheets with a fiber size of approximately 977 μm were prepared by handsheet former.³² The fiber suspensions with fiber sizes of 560, 340, and 177 μm were diluted to a 0.2 wt % consistency in distilled water followed by stirring at 1000 rpm for 15 min. The suspensions were poured into Petri dishes after 10 min of vacuum deaeration and dried at room temperature.

Poly(3,4-ethylenedioxythiophene) was deposited on the yarns using a galvanostatic deposition technique with a current density of 0.8 $\text{A}\cdot\text{m}^{-2}$ at room temperature. The deposition solution was prepared by making a 0.1 M tetrabutylammonium hexafluorophosphate (TBAPF6) solution in 99% propylene carbonate and 1% water, later mixed with 0.1 M EDOT. A pair of 10 mm \times 50 mm sheets of niobium thin foil were used with 1 M sulfuric acid to measure the capacitance per area of niobium. The electrical conductivity of Nb NW yarns is measured by using 4-point probe technique as described in reference 17.

The calculation of volumetric and gravimetric capacitance, and power and energy density of the capacitor were calculated as follows. The volumetric and gravimetric capacitance of the neat Nb NW-based supercapacitors were calculated using $C_m = ((2C_{\text{tot}})/m)$ and $C_v = C_m \times \rho_{\text{Nb}}$, where m is mass of one electrode for the cases of using identical electrodes, and ρ_{Nb} is the density of bulk niobium. The total capacitance was measured using cyclic voltammetry and then using $C_{\text{tot}} = I \times \nu^{-1}$ from the CV curves, where ν is the scan rate and I is the value of the current at the symmetry axis, which was at a potential of 0 V unless stated otherwise. For PEDOT-coated samples, the volume of the one electrode was measured and used to find the value of C_v . In all experiments with PEDOT-coated Nb NWs, symmetrical samples were used; however, for bare Nb NW samples with two electrodes of different masses, the following relation was used to find the capacitance of each electrode:

$$C_1 = C_{\text{tot}}(1 + \gamma)$$

$$C_2 = \frac{C_{\text{tot}}(1 + \gamma)}{\gamma}$$

where γ is the mass ratio (m_1/m_2). For life cycle measurements, the capacitance was found from the slope for the constant current charge and discharge curves using $C_{\text{tot}} = I/(dV/dt)$.

For the generation of the Ragone plot, we calculated the volumetric power density ($P_{V(\text{av})}$, $\text{W}\cdot\text{m}^{-3}$) and the energy density (E_v , $\text{J}\cdot\text{m}^{-3}$) at the device level (V_{tot}) at each scan rate of ν ($\text{V}\cdot\text{s}^{-1}$) by integrating under the cyclic voltammetry curves (during the discharge cycles and initial potential at E_i) as follows:

$$P_{V(\text{av})} = \frac{1}{V_{\text{tot}}E_i} \int_{E_i}^0 IE dE$$

$$E_v = \frac{1}{V_{\text{tot}}\nu} \int_{E_i}^0 IE dE$$

Alternatively, the following equations were used to calculate the peak volumetric power and energy density:

$$E_v = \frac{C_{\text{tot}}E^2}{2V_{\text{tot}}}$$

$$P_v = \frac{E^2}{4R_{\text{ESR}}V_{\text{tot}}}$$

The EIS was performed with EC-Lab software by sweeping one sinusoidal frequency with an amplitude of 20 mV and a DC bias of 0.2 V from 200 kHz to 10 mHz. Poly(vinyl alcohol) (PVA) with sulfuric acid was used for the solid electrolyte-based supercapacitors. Sulfuric acid, DI water, and PVA were mixed with a mass ratio of 1:10:1 and stirred aggressively for 1 h at 90 $^{\circ}\text{C}$.

ASSOCIATED CONTENT

Supporting Information

A video demonstration of supercapacitor design and performance. Documentation on the calculation of specific capacitance, the effects of electrolyte and scanning rate on capacitance, preparation and characterization of low-resistance separators, bare and PEDOT-coated niobium performance, capacitance as a function of diameter and inserted twist, impedance and the effect of solid electrolyte, and the effect of twist and bending on capacitor performance. Figures showing the experimental setup (including the electrode diagram and charging process), energy-dispersive x-ray spectroscopy data, SEM images of nanowires and wood fibers, CV curves for ionic liquid and PEDOT-coated cells, Coloumbic efficiency data, capacitance data, Nyquist plots, and a proposed circuit model and parameters. The Supporting Information is available free of charge on the ACS Publications website at DOI: 10.1021/acsami.5b02327.

AUTHOR INFORMATION

Corresponding Author

*E-mail: seyed@mit.edu, sm.mirvakili@gmail.com.

Author Contributions

S.M.M. proposed the idea; conceived, designed, and performed the experiments and modeling; analyzed data; and wrote the manuscript. M.N.M. designed, fabricated, and characterized the separators and cowrote the manuscript. P.E. contributed expertise on separator design. J.D.W.M. contributed to analysis and modeling. I.W.H. designed experiments and contributed to the analysis. All authors discussed the results and commented on the manuscript.

Notes

The authors declare no competing financial interest.

ACKNOWLEDGMENTS

S.M.M. was supported by a Natural Sciences and Engineering Research Council of Canada (NSERC) Alexander Graham Bell Graduate Fellowship. We thank Mike Chang and Professor Alireza Nojeh for performing the energy-dispersive X-ray spectroscopy. Dr. Ke Han of the National High Field Magnet Laboratory at Florida State University provided the Cu–Nb wire used.

REFERENCES

- (1) Wu, Z. S.; Parvez, K.; Feng, X.; Müllen, K. Graphene-Based In-Plane Micro-Supercapacitors with High Power and Energy Densities. *Nat. Commun.* **2013**, *4*, 2487.
- (2) Kim, T. Y.; Lee, H. W.; Stoller, M.; Dreyer, D. R.; Bielawski, C. W.; Ruoff, R. S.; Suh, K. S. High-Performance Supercapacitors Based on Poly(ionic liquid)-Modified Graphene Electrodes. *ACS Nano* **2011**, *5*, 436–442.
- (3) Lee, J. A.; Shin, M. K.; Kim, S. H.; Cho, H. U.; Spinks, G. M.; Wallace, G. G.; Lima, M. D.; Lepró, X.; Kozlov, M. E.; Baughman, R. H.; Kim, S. J. Ultrafast Charge and Discharge Biscrolled Yarn Supercapacitors for Textiles and Microdevices. *Nat. Commun.* **2013**, *4*, 1970.
- (4) Choi, C.; Lee, J. A.; Choi, A. Y.; Kim, Y. T.; Lepró, X.; Lima, M. D.; Baughman, R. H.; Kim, S. J. Flexible Supercapacitor Made of Carbon Nanotube Yarn with Internal Pores. *Adv. Mater.* **2014**, *26*, 2059–2065.
- (5) Kou, L.; Huang, T.; Zheng, B.; Han, Y.; Zhao, X.; Gopalsamy, K.; Sun, H.; Gao, C. Coaxial Wet-Spun Yarn Supercapacitors for High-Energy Density and Safe Wearable Electronics. *Nat. Commun.* **2014**, *5*, 3754.
- (6) Ren, J.; Li, L.; Chen, C.; Chen, X.; Cai, Z.; Qiu, L.; Wang, Y.; Zhu, X.; Peng, H. Twisting Carbon Nanotube Fibers for Both Wire-Shaped Micro-Supercapacitor and Micro-Battery. *Adv. Mater.* **2013**, *25*, 1155–1159.
- (7) Meng, Y.; Zhao, Y.; Hu, C.; Cheng, H.; Hu, Y.; Zhang, Z.; Shi, G.; Qu, L. All-Graphene Core-Sheath Microfibers for All-Solid-State, Stretchable Fibriform Supercapacitors and Wearable Electronic Textiles. *Adv. Mater.* **2013**, *25*, 2326–2331.
- (8) Wang, K.; Meng, Q.; Zhang, Y.; Wei, Z.; Miao, M. High-Performance Two-Ply Yarn Supercapacitors Based on Carbon Nanotubes and Polyaniline Nanowire Arrays. *Adv. Mater.* **2013**, *25*, 1494–1498.
- (9) Liu, N.; Ma, W.; Tao, J.; Zhang, X.; Su, J.; Li, L.; Yang, C.; Gao, Y.; Golberg, D.; Bando, Y. Cable-Type Supercapacitors of Three-Dimensional Cotton Thread Based Multi-Grade Nanostructures for Wearable Energy Storage. *Adv. Mater.* **2013**, *25*, 4925–4931.
- (10) Fu, Y.; Wu, H.; Ye, S.; Cai, X.; Yu, X.; Hou, S.; Kafafy, H.; Zou, D. Integrated Power Fiber for Energy Conversion and Storage. *Energy Environ. Sci.* **2013**, *6*, 805.
- (11) Yang, X.; Cheng, C.; Wang, Y.; Qiu, L.; Li, D. Liquid-Mediated Dense Integration of Graphene Materials for Compact Capacitive Energy Storage. *Science* **2013**, *341*, 534–537.
- (12) Gogotsi, Y.; Simon, P. True Performance Metrics in Electrochemical Energy Storage. *Science* **2011**, *334*, 917–918.
- (13) Fekri, N.; Madden, J. D. W.; Lee, N. Y.-J.; Ko, F.; Michal, C. A. Influence of Porosity on Charging Speed of Polypyrrole. *Synth. Met.* **2014**, *187*, 145–151.
- (14) Chen, Y.; Du, L.; Yang, P.; Sun, P.; Yu, X.; Mai, W. Significantly Enhanced Robustness and Electrochemical Performance of Flexible Carbon Nanotube-Based Supercapacitors by Electrodepositing Polypyrrole. *J. Power Sources* **2015**, *287*, 68–74.
- (15) Yang, P.; Mai, W. Flexible Solid-State Electrochemical Supercapacitors. *Nano Energy* **2014**, *8*, 274–290.
- (16) Yang, P.; Xiao, X.; Li, Y.; Ding, Y.; Qiang, P.; Tan, X.; Mai, W.; Lin, Z.; Wu, W.; Li, T.; Jin, H.; Liu, P.; Zhou, J.; Wong, C. P.; Wang, Z. L. Hydrogenated ZnO Core-Shell Nanocables for Flexible Supercapacitors and Self-Powered Systems. *ACS Nano* **2013**, *7*, 2617–2626.
- (17) Mirvakili, S. M.; Pazukha, A.; Sikkema, W.; Sinclair, C. W.; Spinks, G. M.; Baughman, R. H.; Madden, J. D. W. Niobium Nanowire Yarns and their Application as Artificial Muscles. *Adv. Funct. Mater.* **2013**, *23*, 4311–4316.
- (18) Zhang, M.; Atkinson, K. R.; Baughman, R. H. Multifunctional Carbon Nanotube Yarns by Downsizing an Ancient Technology. *Science* **2004**, *306*, 1358–1361.
- (19) Yu, D.; Goh, K.; Wang, H.; Wei, L.; Jiang, W.; Zhang, Q.; Dai, L.; Chen, Y. Scalable Synthesis of Hierarchically Structured Carbon Nanotube-Graphene Fibres for Capacitive Energy Storage. *Nat. Nanotechnol.* **2014**, *9*, 555–562.
- (20) Xu, Z.; Sun, H.; Zhao, X.; Gao, C. Ultrastrong Fibers Assembled from Giant Graphene Oxide Sheets. *Adv. Mater.* **2013**, *25*, 188–193.
- (21) Aboutaleb, S. H.; Jalili, R.; Esrafilzadeh, D.; Salari, M.; Gholamvand, Z.; Aminorroaya Yamini, S.; Konstantinov, K.; Shepherd, R. L.; Chen, J.; Moulton, S. E.; Innis, P. C.; Minett, A. I.; Razal, J. M.; Wallace, G. G. High-Performance Multifunctional Graphene Yarns: Toward Wearable All-Carbon Energy Storage Textiles. *ACS Nano* **2014**, *8*, 2456–2466.
- (22) Jalili, R.; Aboutaleb, S. H.; Esrafilzadeh, D.; Shepherd, R. L.; Chen, J.; Aminorroaya-Yamini, S.; Konstantinov, K.; Minett, A. I.; Razal, J. M.; Wallace, G. G. Scalable One-Step Wet-Spinning of Graphene Fibers and Yarns from Liquid Crystalline Dispersions of Graphene Oxide: Towards Multifunctional Textiles. *Adv. Funct. Mater.* **2013**, *23*, 5345–5354.
- (23) Olivares-Navarrete, R.; Olaya, J. J.; Ramirez, C.; Rodil, S. E. Biocompatibility of Niobium. *Coatings* **2011**, *1*, 72–87.
- (24) van Drunen, J.; Kinkead, B.; Wang, M. C. P.; Sourty, E.; Gates, B. D.; Jerkiewicz, G. Comprehensive Structural, Surface-Chemical and Electrochemical Characterization of Nickel-Based Metallic Foams. *ACS Appl. Mater. Interfaces* **2013**, *5*, 6712–6722.
- (25) Futaba, D. N.; Hata, K.; Yamada, T.; Hiraoka, T.; Hayamizu, Y.; Kakudate, Y.; Tanaike, O.; Hatori, H.; Yumura, M.; Iijima, S. Shape-Engineerable and Highly Densely Packed Single-Walled Carbon Nanotubes and their Application as Super-Capacitor Electrodes. *Nat. Mater.* **2006**, *5*, 987–994.
- (26) El-Kady, M. F.; Strong, V.; Dubin, S.; Kaner, R. B. Laser Scribing of High-Performance and Flexible Graphene-Based Electrochemical Capacitors. *Science* **2012**, *335*, 1326–1330.
- (27) Xia, J.; Chen, F.; Li, J.; Tao, N. Measurement of the Quantum Capacitance of Graphene. *Nat. Nanotechnol.* **2009**, *4*, 505–509.
- (28) Nyholm, L.; Nyström, G.; Mhramyan, A.; Strømme, M. Toward Flexible Polymer and Paper-Based Energy Storage Devices. *Adv. Mater.* **2011**, *23*, 3751–3769.
- (29) Dong, Z.; Jiang, C.; Cheng, H.; Zhao, Y.; Shi, G.; Jiang, L.; Qu, L. Facile Fabrication of Light, Flexible and Multifunctional Graphene Fibers. *Adv. Mater.* **2012**, *24*, 1856–1861.
- (30) Pech, D.; Brunet, M.; Durou, H.; Huang, P.; Mochalin, V.; Gogotsi, Y.; Taberna, P.-L.; Simon, P. Ultrahigh-Power Micrometre-Sized Supercapacitors Based on Onion-Like Carbon. *Nat. Nanotechnol.* **2010**, *5*, 651–654.
- (31) Xiao, X.; Li, T.; Yang, P.; Gao, Y.; Jin, H.; Ni, W.; Zhan, W.; Zhang, X.; Cao, Y.; Zhong, J.; Gong, L.; Yen, W.-C.; Mai, W.; Chen, J.; Huo, K.; Chueh, Y.-L.; Wang, Z. L.; Zhou, J. Fiber-Based All-Solid-State Flexible Supercapacitors for Self-Powered Systems. *ACS Nano* **2012**, *6*, 9200–9206.
- (32) Mirvakili, M. N.; Hatzikiriakos, S. G.; Englezos, P. Superhydrophobic Lignocellulosic Wood Fiber/Mineral Networks. *ACS Appl. Mater. Interfaces* **2013**, *5*, 9057–9066.